Engineering and Technology Journal
Journal homepage: engtechjournal.org

Effect of CO_2 Laser Fluence in Cladding Process on the Microstructure of Cold Rolled 0.2 % Carbon Steel

Mohammed J. Kadhim [a], Mahdi M. Hanon [b], Suhair A. Hussein [c]

[a,b,c] Department of Production Engineering and Metallurgy, University of Technology, Baghdad, Iraq
zainzain2011.zz@gmail.com

Submitted: 04/12/2019 Accepted: 18/04/2020 Published: 25/07/2021

K E Y W O R D S

CO_2 Laser Cladding, Microhardness, Cold Rolled 0.2% Carbon Steel, Ni-10 wt% Al.

A B S T R A C T

In this article a 1.8kW continuous wave of high power CO_2 laser was used to clad of a titular composition of Ni – 10 wt% Al powder on cold rolled 0.2% carbon steel substrate. The feed rate was kept constant after many preliminary claddings at approximately 11 g/min. In order to produce clads with different specific energies and interaction times, different traverse speeds were used in the range of 1.5 to 12.5 mm/s. The microstructure of substrate was changed at the heat affected zones under the variety of specific energies. The cladded coatings showed the presence of γ solid solution and β (NiAlFe) phases. A strong metallurgical bonding produced between the substrate and the clad coat at fluence higher than 48 J/mm2. The changing in microstructure were observed using both microscope and SEM. The microhardness was evaluated using Vicker's microhardness test. The microstructure of the substrate was ferrite and pearlite transformed to martensite at the region adjacent to the clad interface. It followed by a three regions can be classified, a grain growth zone (large grains of austenite/ferrite and pearlite), recrystallization zone (fine grains of austenite/ferrite and pearlite) and recovery zone (the structure has a little changes from the structure of low carbon steel). The microhardness testing result showed higher values for the clad regions compared with substrate. This study emphasize the possibility to develop a temporary new graded material.

How to cite this article: M. J. Kadhim, M. M. Hanon, S. A. Hussein, "Effect of CO_2 Laser Fluence in Cladding Process on the Microstructure of Cold Rolled 0.2 % Carbon Steel," Engineering and Technology Journal, Vol. 39, No. 07, pp. 1052-1059, 2021.
DOI: https://doi.org/10.30684/etj.v39i7.1475

1. INTRODUCTION

Laser cladding can be defined as a melting process in which the laser beam induced to fuse an alloy addition on to a substrate (base material) producing a homogeneous surface with a strong metallurgical bonding on the substrate with very low dilution[1]. Cladding improvement surface properties by selecting an alloy with a good wear, erosion, and oxidation or corrosion resistance fittings required properties. Laser cladding has unique properties made it important in the industrial

processing, namely high input energy, low distortion, avoidance of undesirable phase transformations and minimum dilution between the substrate and the coating, great processing flexibility , possibility of selectively cladding small areas, high products quality and also economic benefits [2]. Most substrates that appropriate for laser cladding are stainless steels, carbon–manganese and alloys based on Al, Ti, Mg, Cu and Ni. Widespread of alloys for cladding are based on cobalt, iron and nickel. Maybe, they include tungsten carbides, Ti and Si, ceramics like Zr that brews a reinforced particle composite metal matrix surface by solidification which giving more resistance for wear. Laser cladding process is the choice of many fields including covering, reform and reworking.

Yellup [3] revealed that the laser steel device among another covering with very low dilution, high solidity and structures are fine. Additionally, Mazumder [4] have demonstrated the likelihood to assemble a three dimensional part from tool steel (H13) utilizing the purported direct system of metal deposition which is a progressed system cladding laser with coaxial powder blowing. Reparation of molds, which have encountered a serious harm amid their lifetime administration by high speed steel laser cladding with a high content of molybdenum, was announced by Navas [5]. Abrasive wear conducts a few cladding laser device coatings of steel considered in the work by Wang [6] who demonstrated the track of laser covering results in various features inside the reheated region in correlation with a region when material exists in the clad condition.

Today, the increasing demand to the cladding laser backs to laser peerless advantages, high conductivity, automation eligibility, non-contact operating, removal finishing processing, reduce processing cost, efficiency of product quality, high materials exploitation. Steel is the most generally utilized material for apparatuses, shafts, railroad wheels, etc. in numerous mechanical applications, and the market interest for the fixing of such items is enormous. Along these lines, it is direly important to locate a successful fix strategy to re-establish the geometry and give adequate solidarity to such parts taking into consideration their proceeded with the use [7]. This method is utilized for depositing alloys on turbine sharp edges, motor valves, valve seats and boring parts.

The most important goal of this research is using a cheap substrate with lower properties such as cold rolled 0.2 wt% carbon steel and cladding it with Ni-Al powder injection using high power carbon dioxide laser system to enhance the substrate properties. Also, obtain a better microstructure of the substrate after using laser cladding process make it more protected. On the other hand, study and analyze changing in the microstructure and how affecting it in the improvement of microhardness cladding areas.

2. EXPERIMENTAL PROCEDURES

A 1.8 kW continuous, fast axial, shock stabilized, gas discharged CO_2 laser model BOC 901 which was designed by British Oxygen Company and manufactured by Control Laser Ltd. used to clad the samples. The laser beams of 10.6 μm wave length is produce from the mixture of CO_2, He and N_2 gases entered the four tubes. Flat plates of cold rolled 0.2 wt% carbon steel of thickness 6 mm, width 30 mm and length 60 mm were used as substrate for laser cladding. The substrates were sand blasted to produce a relatively rough surface of approximately 10 μm CLA roughness to enhance the absorption. The clad powder used is a thoroughly mixture of 90 wt% Ni and 10 wt% Al. The average particle size of Ni and Al powders are 106 and 250 μm, respectively. The steel substrate was mounted rigidly on x-y movable table by using suitable jigs perpendicular to the stationary laser beam. The selected laser beam diameter of 3 mm was achieved by selecting the suitable perpendicular distance to the laser beam by using the formula described by Mohammed [8].

The cladding premixed powder was injected directly by using a continuous feeder to the laser melt pool. The powder was injected from copper tube with nozzle diameter 3 mm at a distance of approximately 10 mm from the melt pool with 30^o with the substrate (Figure1). The feed rate was kept constant after many preliminary claddings at approximately 11 g/min. In order to produce clads with different specific energies and interaction times, different traverse speeds were used (1.5, 3.6, 5, 7.1, 8.6, 12.5) mm/s (Table I). The laser power used to produce a high power density suitable for laser cladding (power/laser beam area) and different specific energies is 1.8 kW. The laser mode tuned is near TEM00.

In order to evaluate the behavior of clads for all performances, transverse sections should be prepared. The clad samples were cut by wire cutting transversally and then grinding with 220, 500 and 1000 SiC grid emery papers respectively and then polished with 1μm diamond paste and dried. Two etching solutions were used to evaluate the microstructure of (i) substrate and heat affected

zones; Nital (98% Alcohol +2%HNO_3) and (ii) the cladding area with 3ml HCl, 2mlHNO_3 and 0.1 ml glycerin. The microstructure of samples and the dimensional geometries of cladding regions were studied and evaluated by using optical microscope and (SEM) type vega3 tescan. The microhardness testing evaluated by Digital micro Vickers hardness tester TH714.

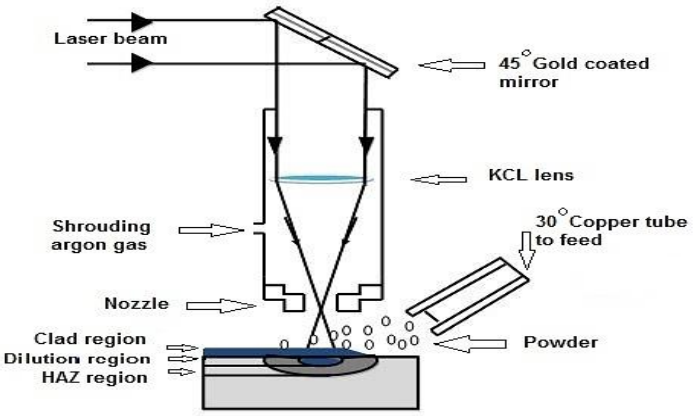

Figure 1: Some laser cladding system components.

TABLE I: The most important parameters of cladding process

Parameters	Values
TEM_{mn}	00
Raw laser beam diameter	20 mm
Focal length	125 mm
Shrouding gas ,Argon	2.2 SLPM
Laser power (P)	1.8 kW
Diameter of laser beam (d)	3mm
Speed of Traverse (V)	1.5 -12.5 mm/s
Interacton time (t)	0.24-2 s
Power density ($4P/\pi d^2$)	255W/mm^2
Fluence (P/dv)	48-400 J/mm^2

3. RESULTS AND DISCUSSION

The microstructure of substrate (as received) before laser cladding includes both ferrite (α) and pearlite (p) phases as shown in Figure 2.

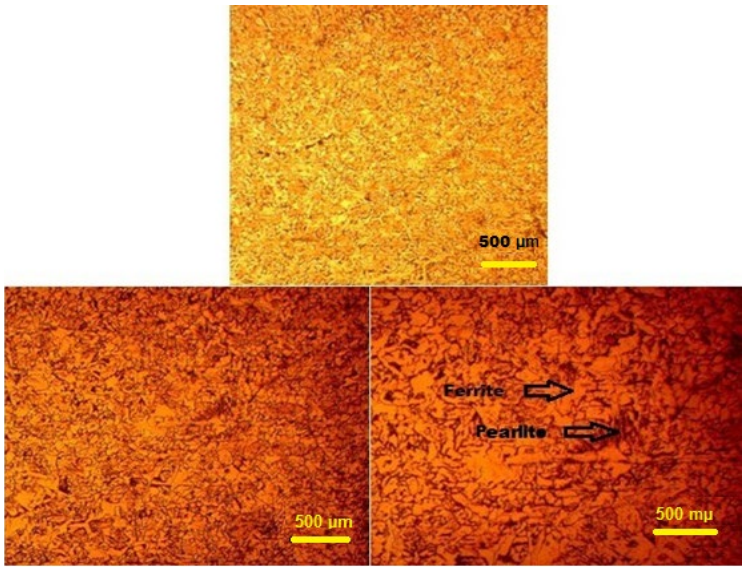

Figure 2: The microstructure of the substrate that containing both ferrite and pearlite.

It was seen that there are no defects or cracking in the different cross sections of cladding areas. Also, various geometrical measurements were obtained at different fluence values [9] (400, 167, 120, 85, 70, and 48 J/mm^2). The cladding regions variation appears obviously in Figure 3.

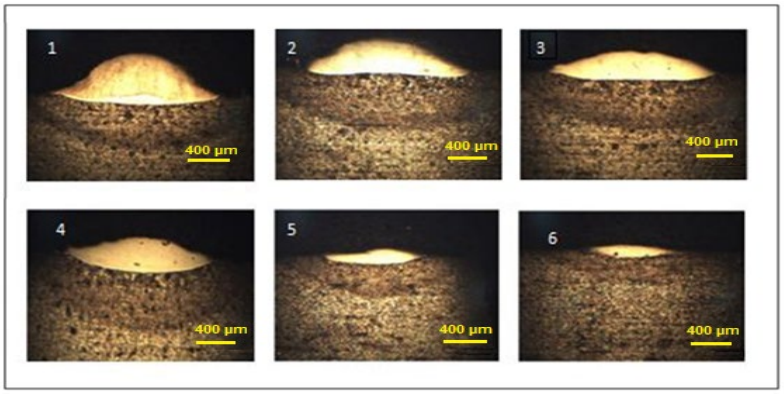

Figure 3: The cross-section of cladding regions showing the different geometrical dimensions at fluence (J/mm^2): (1)400, (2)167, (3)120, (4)85, (5)70, and (6) 48.

The microstructure of cold rolled 0.2wt% carbon steel was ferrite and pearlite transformed near the interface region (between cladding area and the substrate) to four distinct zones within the heat affected zone areas appeared in optical microscope and can be classified into martensite zone (near the interface), grain growth zone (below martensite zone), recrystallization zone (below grain growth zone) and finally the recovery zone (at the interface between recrystallization and substrate). The chemical composition changes from the higher region of the clad to the preposition of the interface because of the dilution of clad region from steel, as shown in Figure 4 [10]. The formation of martensite zone was due to the rapid cooling from the austenitic range, as shown in Figure 5. This makes it have higher microhardness than grain growth and the other regions of heat affected zone.

The nearness of certain grains of austenite is because of the lower dispersion time which wasn't adequate to create too homogenous soaking of carbon in austenite. This was affirmed from the microstructure because of the non-attendance equiaxed and interconnected grains related with ferrite. In the grain growth zone, there is relatively large austenite/ferrite and perlite. In the recrystallization zone, there are fine austenite/ferrite and pearlite grains with microhardness higher than grain growth due to fine grains. Finally, in the recovery zone, the structure has little changes from the structure of low carbon steel. The temperatures become less when turning towards the substrate. Underneath the martensitic zone, the temperature proposed to be under 1000°C and may be under 300°C close to the substrate. In spite of the short interaction time, it was adequate to all these heat treatments (samples) to show grain growth, recrystallization and recovery zone clearly, because of the high input energy in the deformed substrate. Higher temperatures underneath to the temperature of martensitic change are adequate to create the grain growth of the distorted microstructure. Accordingly, the microstructure is comprised of a limited quantity of austenite, ferrite and pearlite, as shown in Figure 6 [11]. It's observed from the microstructure of cladding area (Figure 7) that the all phases based on the Ni solid solution contain a distinctive amount of iron and aluminum. Regardless of the laser processing parameters that used in the cladding process, these phases are generally Ni solid solution (γ)/Ni_3Al (γ`) and intermetallic compound dependent on NiAlFe ($\beta$). And, the amount of ($\gamma$) phase is little compared with ($\gamma$`) phase [12].

The microstructure of the cladding areas is a cell structure because of the rapid cooling rates. These high cooling rates are due to the rapid solidification and increase the heat transfer by conduction with the substrate. The microstructure of clad region contains β and γ`precipites in the matrix of γ, as shown in Figure 7.

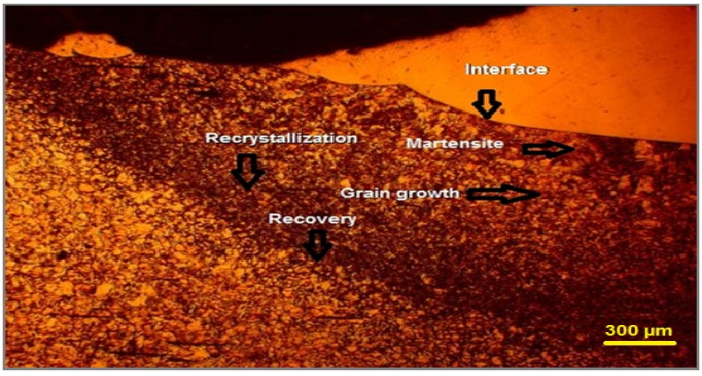

Figure 4: The regions of heat affected zone in addition to the interface.

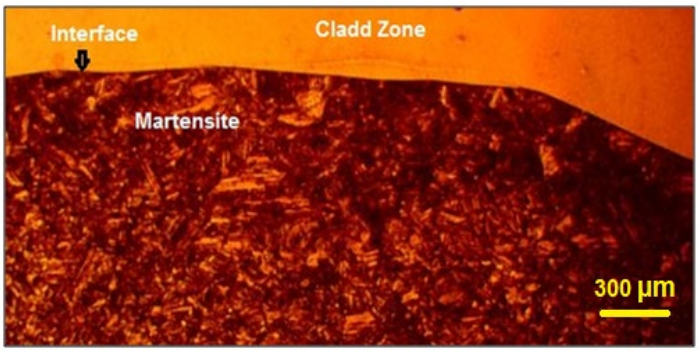

Figure 5: The optical micrograph of the microstructure of martensitic zone.

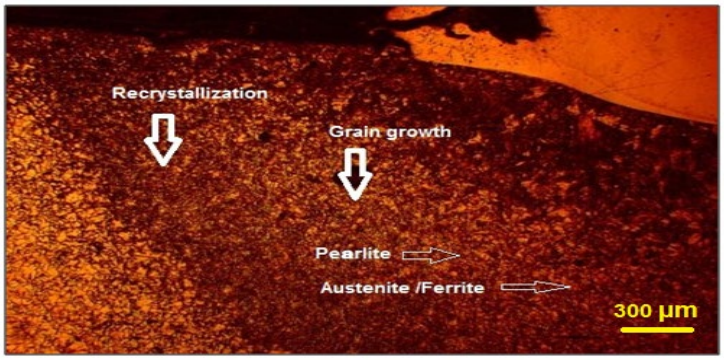

Figure 6: The microstructure comprised of a limited quantity of austenite, ferrite and pearlite.

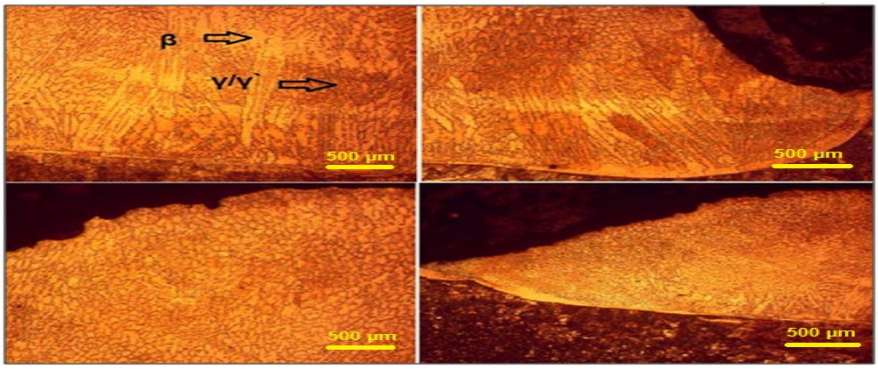

Figure 7: Optical micrograph of the microstructure for clad region.

Microhardness measurements for all cladding regions (near the surface of cladding, center of cladding and the interface) (Figure 8) showed considerable increases in microhardness compared with the substrate sample only. The value of microhardness was about (116) HV for the substrate.

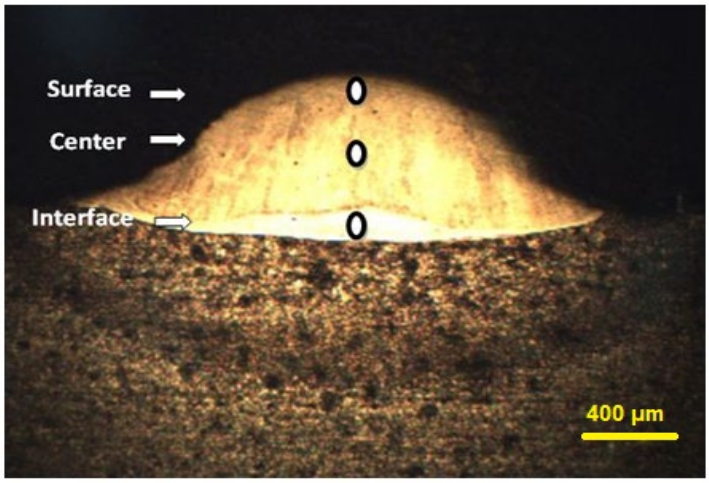

Figure 8: The locations of the applying load in microhardness test.

The microhardness readings for cladding regions are shown in Table II. As seen in this table, the microhardness of all clad regions was higher than the microhardness of the substrate. The microhardness of the interface is lower than the microhardness of the center and the surface of cladding; this is due to the dilution with the substrate [13]. At higher fluence (400J/mm^2), the microhardness was171 HV near the surface and 162 HV at the center of cladding and the interface. On the other hand, the microhardness of the interface, center and the surface of cladding area for all samples decreased as specific energy was increased, as shown in Figure 9. This is due to the microstructure of cladding region changing from the chemical composition of the injected powder from the upper of area cladding surface toward the interface at different specific energies. This manner is due to the dilution of the cladding zone with the steel substrate [14]. EDS analysis proved, that the center of the substrate region mainly containing from Fe while the region near the interface composed from Fe, Ni and Al (Figure 10). SEM analysis showed the details of the upper cladding region (Figure 11).

TABLE II: The microhardness measurements at different regions

Samples No.	Fluence J/mm^2	Near the surface HV	At the center HV	At the Interface HV
1	400	171	171	162
2	167	224	224	211
3	120	248	307	288
4	85	270	242	191
5	70	248	183	183
6	48	258	207	247

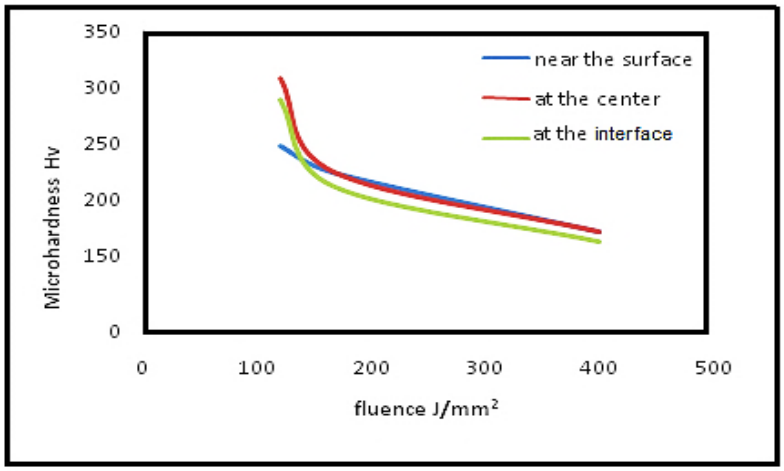

Figure 9: Relationship between microhardness and fluence for all samples groups.

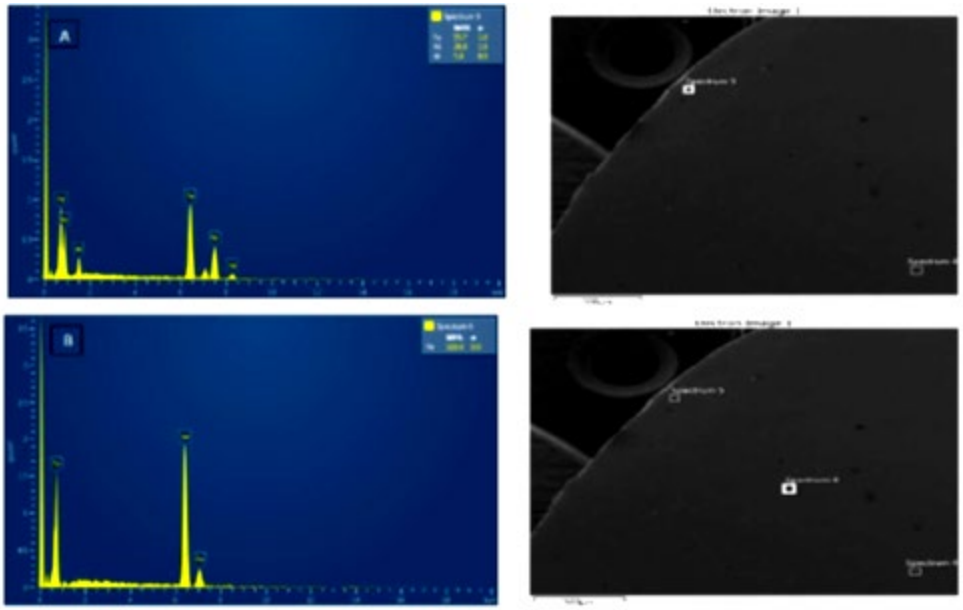

Figure 10: ED's analysis: A- near the interface B- the center of substrate.

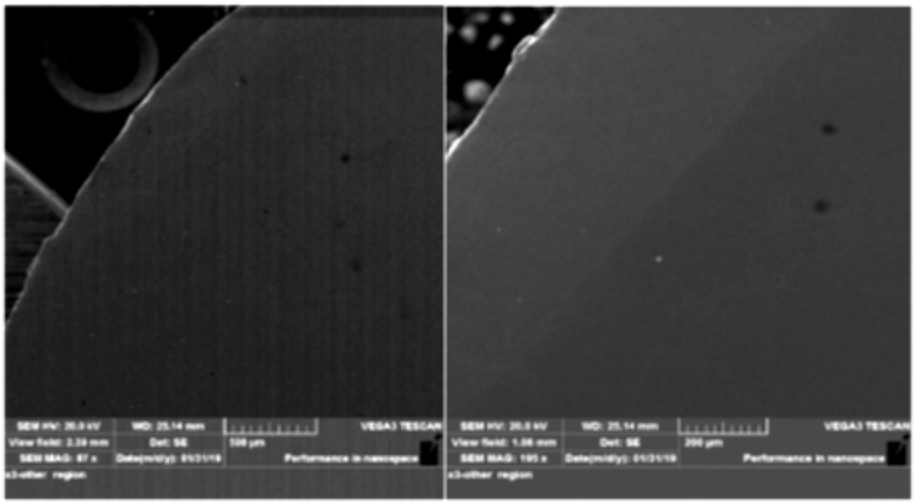

Figure 11: SEM micrographs of the upper cladding coating.

4. CONCLUSIONS

1) Microhardness of cladding areas varies according to the laser cladding parameters that was used.
2) The microhardness decreased as the fluence increased.
3) The microstructure of the substrate was ferrite and pearlite transformed to ferrite, pearlite and austenite after laser cladding at the heat affected zone.
4) At the interface of cladding region, the microstructure composed of Ni-Fe-Al instead of Ni-Al only.

References

[1] J. Liu, J. Li, X. Cheng, H. Wang, Effect of dilution and macro segregation on corrosion resistance of laser clad AerMet100 steel coating on 300M steel substrate, Surf. Coat. Technol., 325 (2017) 352-359. https://doi.org/10.1016/j.surfcoat.2017.04.035

[2] H. Zhang, K. Chong, W. Zhao, Z. Sun,Laser cladding in-situ micro and sub-micro/nano Ti-V carbides reinforced Fe-based layers by optimizing initial alloy powders size, Mater. Lett., 220 (2018) 44-46. https://doi.org/10.1016/j.matlet.2018.02.130

[3] J. M. Yellup, Laser cladding using the powder blowing technique, Surf. Coat. Technol, 7(1995) 121-128, 1995. https://doi.org/10.1016/0257-8972(94)01010-G

[4] C. Young, Design and Validation of Innovative Grid Channel for Injection Mold Cooling, M.Sc. Thesis, Dept. of Mechanical and Aerospace Eng., Univ. of California, Davis, 2018.

[5] C. Navas, A. Conde, B. Fernandez, and F. Zubiri, Laser coatings to improve wear resistance of mould steel, Surf. Coat. Technol, 194 (2005) 136-142. https://doi.org/10.1016/j.surfcoat.2004.05.002

[6] S. H. Wang, J. Y. Chen, L. Xue, A study of abrasive wear behavior of laser-clad tool steel coatings, Surf. Coat. Technol, 200 (2006) 3446-3458, 2006. https://doi.org/10.1016/j.surfcoat.2004.10.125

[7] M. Alam, A. Kaplan, J. Tuominen, and P. Vuoristo, Analysis of the stress raising action of flaws in laser clad deposits, Mater. Des., 46 (2013) 328-337. https://doi.org/10.1016/j.matdes.2012.10.010

[8] M. J. kadhim, Laser cladding of ceramics and sealing of plasma sprayed zirconia based thermal barrier coatings, PhD Thesis, Dept. of Materials, Univ. of Imperial Collage, London, 1990.

[9] R. Awasthi, S. Kumar, K. Chandra, Effect of specific energy input on microstructure and mechanical properties of nickel-base intermetallic alloy deposited by laser cladding, Metall. Mater. Trans. A, 43(2018) 4688-4702.

[10] M. A. A. Bash, A. M. Mustfa, A. M. Resan, F. F. Sayyid, Microstructure and microhardness of laser cladding Ni based on cold rolled steel, Iraqi J. Mech. Mater. Eng. , Vol. 18(2018) 201-213.

[11] F. C. Cerda, C. Goulas, I. Sabirov, Microstructure, Texture and mechanical properties in allow carbon steel after ultrafast heating, Mater. Sci. Eng.: A, 672(2016) 108-120. https://doi.org/10.1016/j.msea.2016.06.056

[12] M. Bash, Effect of feed rate on laser surface cladding of cold rolled carbon steel, Eng. Technol.J., 35 (2017) 922-929.doi: 10.30684/etj.35.9A.9

[13] S. Gnanasekaran, G. Padmanaban, and V. Balasubramanian, Effect of laser power on metallurgical, mechanical and tribological characteristics of hardfaced surfaces of nickel-based alloy, Lasers Manuf. Mater. Process., 4 (2017) 178-192. https://doi.org/10.1007/s40516-017-0045-z

[14] J. Lei, C. Shi, S. Zhou, L. C. Zhang, Enhanced corrosion and wear resistance properties of carbon fiber reinforced Ni-based composite coating by laser cladding, Surf. Coat. Technol, 334 (2018) 274-285. https://doi.org/10.1016/j.surfcoat.2017.11.051